Condensed Matter Physics, 2003, Vol. 6, No. 2(34), pp. 325–332

CONDENSED MATTER PHYSICS

Luminescent kinetic characteristics of $CsPbCl_3$ aggregates dispersed in $Rb_{1-x}Cs_xCl$ ($x = 0.05 \div 0.2$) matrices

S.Myagkota*, A.Gloskovskii, R.Gladyshevskii, A.Voloshinovskii

Ivan Franko National University of Lviv,
8 Kyryla i Mefodiya Str., 79005 Lviv, Ukraine

Received April 21, 2003

The luminescent kinetic parameters of the $CsPbCl_3$ nanocrystals dispersed in matrices of solid solutions $Rb_{1-x}Cs_xCl$ ($x = 0.05 \div 0.2$) were studied under pulse synchrotron radiation excitation. Formation of $CsPbCl_3$ nanocrystals is confirmed by manifestation of the quantum size effect, which is displayed by a short-wave shift of the exciton luminescence maximum and an essential shortening of the luminescence decay time for of $CsPbCl_3$ nanocrystals as compared to that for an excitonic luminescence of a bulk single crystal $CsPbCl_3$. For the first time, using the atomic force microscopy method, the lead-containing nanocrystals embedded in a matrix of the $Rb_{0.95}Cs_{0.05}Cl$ solid solution have been directly observed.

Key words: *nanocrystal, quantum size effect, luminescent kinetic parameters, topology of crystal cleavage surface, atomic force microscopy*

PACS: *32.50.+d, 87.15.Mi, 78.60.-b, 33.50.-j*

1. Introduction

Along with the familiar semiconducting nanocrystals of the CdS, CdSe, CuCl, PbI_2 type, recently the ionic lead-containing crystals of the $CsPbX_3$ (X = Cl, Br, I) type have been extensively studied. Some of them are characterized by a high intensity of luminescence with short decay times (tens of picoseconds) [1]. Such luminescent parameters make these materials prospective for the development of fast detectors of high-energy irradiation.

The $CsPbX_3$ (X = Cl, Br, I) nanocrystals are formed in the insulating haloid matrices with different crystal structures activated by ions of lead or cesium, after a prolonged (10÷100 h) high-temperature (150÷250 °C) annealing. The formation of nanocrystals has been confirmed by manifestation of the quantum size effect in their spectral luminescent characteristics [1–4]. High efficiency of the luminescent

*E-mail: lumi@franko.lviv.ua

method of identifying the crystal type and nanocrystal sizes in the dielectric matrix has been analyzed in [5].

Lead-containing nanocrystals formed in the matrices having the CsCl crystal structure were directly observed only in the studies of the surface of thin films $CsX:PbX_2$ (X = Cl, Br, I) using the atomic force microscopy (AFM) method [6–8].

In the present paper we study the luminescent kinetic characteristics of the $CsPbCl_3$ nanocrystals embedded in the matrix of $Rb_{1-x}Cs_xCl$ ($x = 0.05 \div 0.2$) solid solutions. The crystal structure of the solid solutions $Rb_{1-x}Cs_xCl$ is of the NaCl type, since the content of CsCl in $Rb_{1-x}Cs_xCl$ is smaller than $x = 0.33$. According to the results of the theoretical calculations, at this content of the BX impurity, the structure type of the solid solution $A_{1-x}B_xX$ is the same as that of the major component AX [9]. Using the AFM method we directly observe the lead-containing nanocrystals dispersed in the matrices of the $Rb_{1-x}Cs_xCl$ ($x = 0.05 \div 0.2$) solid solutions. In these studies the crystals with cleaved surfaces are used, which makes them more advantageous compared to the thin film studies [6–8] where observation of nanocrystals is distorted by the thin film structure.

Let us note that the formation of the $CsPbCl_3$ type nanocrystals embedded in a crystalline structure of NaCl type has not been observed yet. It was established only for NaCl crystals activated by lead that the increase of the storage time of the crystal, of the annealing temperature or of the impurity content leads to the formation of the Pb-containing aggregates $PbCl_2$-type embedded in the NaCl matrix [10].

2. Experiment

The $Rb_{1-x}Cs_xCl$–Pb ($x = 0.05 \div 0.2$) crystals ($C_{Pb} = 1$ mole% in the melt) were grown by the Stockbarger method in two stages. First the $Rb_{1-x}Cs_xCl$ ($x = 0.05 \div 0.2$) crystal matrix, and then the $Rb_{1-x}Cs_xCl$–Pb crystal were grown. In order to form the $CsPbCl_3$ nanocrystals dispersed in the $Rb_{1-x}Cs_xCl$ ($x = 0.05 \div 0.2$) matrix, the $Rb_{1-x}Cs_xCl$–Pb ($x = 0.05 \div 0.2$) crystals were subjected to a prolonged (100 h) high-temperature ($T = 200$ °C) annealing.

The luminescent kinetic characteristics of the crystals were measured using the time resolved spectroscopic methods at the SUPERLUMI station in HASYLAB (Hamburg, Germany). The crystal was excited by synchrotron radiation passed through a normal incidence 2 m vacuum monochromator (spectral width of the slit was about ~ 0.2 nm). The luminescence of the crystal located on the crystal holder of a helium cryostat was detected by a photomultiplier through a secondary B&M monochromator. The luminescence decay kinetics was studied under the pulsed synchrotron excitation (the pulse duration was ≈ 0.12 ns, the repetition period was 480 ns) in the statistical single-photon counting regime with time-to-amplitude conversion. The time instrumental response on the drop of the pulse was 0.4 ns. Actual luminescence decay times were determined with taking into account the shape of the excitation pulse and using the deconvolution procedure. According to [11], the iteration method used for the evaluation of one-exponent parameters of the decay time curve gives a satisfactory accuracy of approximation. Minimal time

constants that can be estimated by this procedure are 0.15 ns. Luminescence spectra were measured within a time window $\Delta t = 5$ ns without delay with respect to the excitation synchrotron pulse. The experimental setup is described more in detail in [12].

Topology of the $Rb_{0.95}Cs_{0.05}Cl$–Pb crystal cleavage surface was explored using the AFM method.

3. Experimental results and discussion

The photoluminescence spectra of the $Rb_{0.95}Cs_{0.05}Cl$–Pb and $Rb_{0.8}Cs_{0.2}Cl$–Pb crystals, excited in the matrix transparency region ($\lambda_{exc} = 310$ and 240 nm) beyond the absorption bands of single lead centers, and the luminescence spectrum of the $CsPbCl_3$ single crystal are given in figure 1.

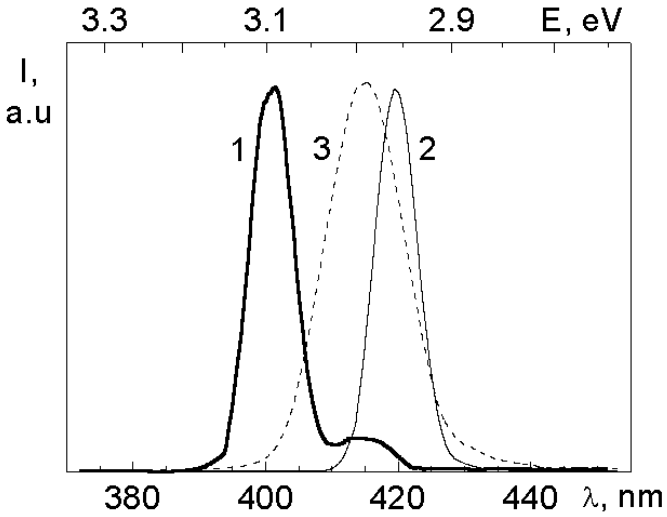

Figure 1. Luminescence spectra of the $CsPbCl_3$ nanocrystals in $Rb_{0.95}Cs_{0.05}Cl$–Pb (curve 1), $Rb_{0.8}Cs_{0.2}Cl$–Pb (curve 3) crystals excited in the matrix transparency region ($\lambda_{exc} = 310$ and 240 nm) and the luminescence spectrum of the $CsPbCl_3$ bulk single crystal at $\lambda_{exc} = 310$ nm (curve 2); $T = 10$ K.

The relatively narrow band with the half-width $\Delta H = 0.04$ eV and maximum at $\lambda_{max} = 408.0$ nm (figure 1, curve 1) of the $Rb_{0.95}Cs_{0.05}Cl$–Pb crystal is similar to the free exciton emission band of the $CsPbCl_3$ single crystal ($\lambda_{max} = 419.6$ nm, $\Delta H = 0.025$ eV) (figure 1, curve 2), the spectral position of which does not depend on the wavelength of the excitation light. Such a similarity of the spectral characteristics is confirmed by the fact that during the high-temperature annealing in the $Rb_{0.95}Cs_{0.05}Cl$–Pb crystal, the lead-containing aggregates of the $CsPbCl_3$ type dispersed in this matrix are formed.

The formation of such aggregates in the $Rb_{1-x}Cs_xCl$–Pb ($x = 0.05 \div 0.2$) crystalline matrices, where the Rb^+, Cs^+ ions and, respectively, the impurity ion Pb^{2+} are characterized by a sixfold surrounding of Cl^- anions, seems logical, since the for-

mation of the $[PbCl_6]^{4-}$ octahedron does not require any structural reconstruction, unlike the crystalline matrices of the CsCl type, where the eightfold surrounding of the Cl^- anions must be changed to a sixfold surrounding in order to create the cluster in the form of $CsPbCl_3$ molecule. The $[PbCl_6]^{4-}$ octahedron is the basis of a $CsPbCl_3$ molecular cluster. Therefore, its presence in the matrix assists the microcrystals of the $CsPbCl_3$ type in the $Rb_{1-x}Cs_xCl$–Pb crystals. Also, the presence of the charge-compensation vacancy v_c^- next to the activator Pb^{2+} ion, facilitates the Pb^{2+} ions mobility with the further formation of the lead-containing aggregates.

The short-wave shift of the emission band maximum of the $CsPbCl_3$ nanocrystals in the $Rb_{0.95}Cs_{0.05}Cl$ matrix ($\lambda_{max} = 408.0$ nm) with respect to the position of the maximum of free exciton emission band of the $CsPbCl_3$ single crystal by $\Delta E = 84$ meV can be interpreted as a manifestation of the quantum size effect. Using the relation between the magnitude of the short-wave shift and the average radius R_{QD} of the nanocrystal [13]

$$\Delta E = \frac{\hbar^2 \pi^2}{2\mu R_{QD}^2}, \tag{1}$$

where $\mu = 0.65$ m_0 [14,15] is the exciton reduced mass for the $CsPbCl_3$ single crystal (m_0 is the mass of a free electron), we determine the average radius of the $CsPbCl_3$ type nanocrystals dispersed in the $Rb_{0.95}Cs_{0.05}Cl$ matrix ($R_{QD} \approx 2.8$ nm). According to theoretical calculations, the quantum size effect is displayed in the aggregates when $R_{QD} < 10r_{exc}$ [16]. Taking into account the numerical value of the exciton radius ($r_{exc} = 9.8$ Å [15] for $CsPbCl_3$), the obtained value of the average radius of the nanocrystals R_{QD} satisfies the condition for the quantum size effect manifestation.

An increase of the luminescence band half-width of the $CsPbCl_3$ aggregates dispersed in the $Rb_{0.95}Cs_{0.05}Cl$ matrix as compared to that of the $CsPbCl_3$ single crystals can be explained by the formation of the $CsPbCl_3$ nanocrystals of different sizes, embedded in the $Rb_{0.95}Cs_{0.05}Cl$ matrix.

The average sizes of the $CsPbCl_3$ nanocrystals formed during the similar high-temperature annealing in the $Rb_{0.95}Cs_{0.05}Cl$–Pb ($C_{Pb} = 1$ mole%) and CsCl–Pb ($C_{Pb} = 1$ mole%) crystals [17] are $R_{QD} \approx 2.8$ and 4.7 nm, respectively. This relation between the dimensions of nanocrystals in the $Rb_{0.95}Cs_{0.05}Cl$ and CsCl matrices is explained by the fact that on decreasing the number of the Cs^+ ions in the compound, the probability of the $CsPbCl_3$ nanocrystals formation in the $Rb_{0.95}Cs_{0.05}Cl$ matrix decreases. On the other hand, at the increased number of Cs^+ ions in the $Rb_{1-x}Cs_xCl$ crystalline solution from $x = 0.05$ to $x = 0.2$, the $CsPbCl_3$ nanocrystals formed in the $Rb_{0.8}Cs_{0.2}Cl$ matrix are larger than in the $Rb_{0.95}Cs_{0.05}Cl$ matrix. Really, the calculated from (1) average radius of the $CsPbCl_3$ nanocrystals formed in the $Rb_{0.8}Cs_{0.2}Cl$–Pb crystal at the same high-temperature annealing as in the case of $Rb_{0.95}Cs_{0.05}Cl$–Pb, equals 4.7 nm. The luminescence maximum of the $CsPbCl_3$ nanocrystals in the $Rb_{0.8}Cs_{0.2}Cl$ matrix with $\lambda_{max} = 415$ nm (figure 1, curve 3) is shifted to the long-range side with respect to the luminescence maximum $\lambda_{max} = 408$ nm for the $CsPbCl_3$nanocrystals dispersed in $Rb_{0.95}Cs_{0.05}Cl$. Coincidence of the values of the average radii of the $CsPbCl_3$ nanocrystals formed

in $Rb_{0.8}Cs_{0.2}Cl$–Pb (C_{Pb} = 1 mole%) and in CsCl–Pb (C_{Pb} = 1 mole%) after the identical high-temperature annealing procedures indicates that the slowing down formation of the $CsPbCl_3$ nanocrystals due to the reduced number of the Cs ions in $Rb_{0.8}Cs_{0.2}Cl$ (as compared to that in CsCl) is compensated by the presence of the $[PbCl_6]^{4-}$ octahedrons in the $Rb_{0.8}Cs_{0.2}Cl$ matrix which causes its acceleration.

Conclusions about the presence of the quantum size effect of the $CsPbCl_3$ nanocrystals are confirmed by the data concerning their luminescence decay kinetics. The luminescence decay time of the $CsPbCl_3$ nanocrystals, dispersed in $Rb_{0.95}Cs_{0.05}Cl$–Pb crystals excited in the matrix transparency region, is described by an exponent with the main decay time τ = 0.15 ns, whereas the kinetics of the luminescence decay in the $CsPbCl_3$ single crystal, excited in the same spectral range, is described by the exponent with the decay time τ = 0.48 ns. Thus, the main decay time of the nanocrystal luminescence band is essentially smaller than the main decay time of the excitonic luminescence of a $CsPbCl_3$bulk single crystal. Shortening of the luminescence decay time in the nanocrystals gives more evidence for the presence of the quantum size effect.

Along with the quantum size effect that changes the luminescent parameters, the matrix exerts a hydrostatic pressure on the nanocrystals. This pressure arises due to the difference between the linear thermal expansion coefficients of the matrix and of the nanocrystals, as well as due to a certain stress acting on the $CsPbCl_3$ nanocrystals at their embedding into a matrix.

In the presence of such a stress, the unit cell constants of the $CsPbCl_3$ nanocrystals are decreased, but the excitonic reflectance peak and the intrinsic emission spectrum of the nanocrystal are shifted to the long-wave region, which is not characteristic of several other crystals. Such an anomalous shift in the $CsPbCl_3$ is well seen in the temperature dependences of the spectral position of the excitonic reflectance peak and of the resonance excitonic luminescence band of a $CsPbCl_3$ single crystal in the $77 \div 4.2$ K temperature range. Namely, when the temperature is lowered and the lattice constant decreases, the excitonic reflectance peak and the luminescence band of the $CsPbCl_3$ single crystal are shifted to lower energies [15]. Hence, the hydrostatic pressure on the nanocrystals does veil the manifestation of the quantum size effect for $CsPbCl_3$ nanocrystals.

By making use of the AFM method we explored the topology of the cleavage surface of the $Rb_{0.95}Cs_{0.05}Cl$–Pb crystal (figure 2).

Space picture of Pb-based nanocrystals placed on the cleavage surface of the $Rb_{0.95}Cs_{0.05}Cl$–Pb crystal is shown in figure 3.

The size of $CsPbCl_3$ nanocrystals in the scanning plane is distorted due to the so-called tip convolution effect. This effect appears due to a certain diameter of the scanning tip ($\approx$ 50 nm). Usually, it overestimates the linear size of nanocrystals. Therefore, only z-component of nanocrystal is reliable. The accuracy of determining the linear dimensions of nanocrystals on a z-axis is 0.5 nm. Finally, the size of $CsPbCl_3$ nanocrystals in the crystal matrix may be estimated in the region of 4–30 nm.

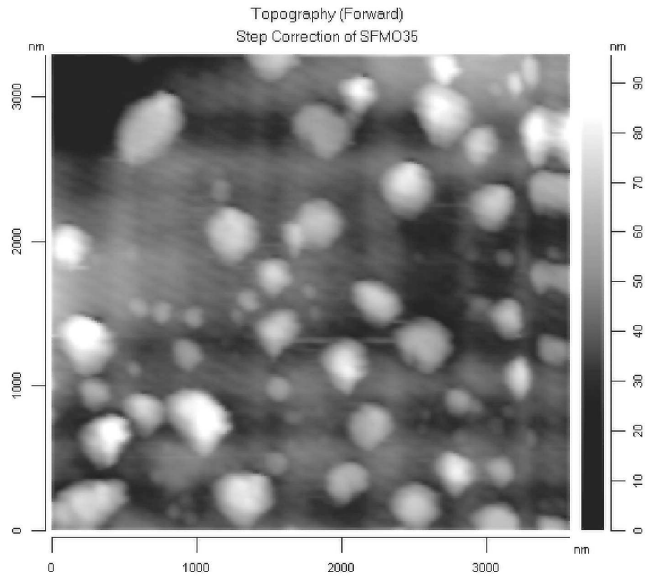

Figure 2. AFM picture of the $Rb_{0.95}Cs_{0.05}Cl$–Pb crystal cleavage surface.

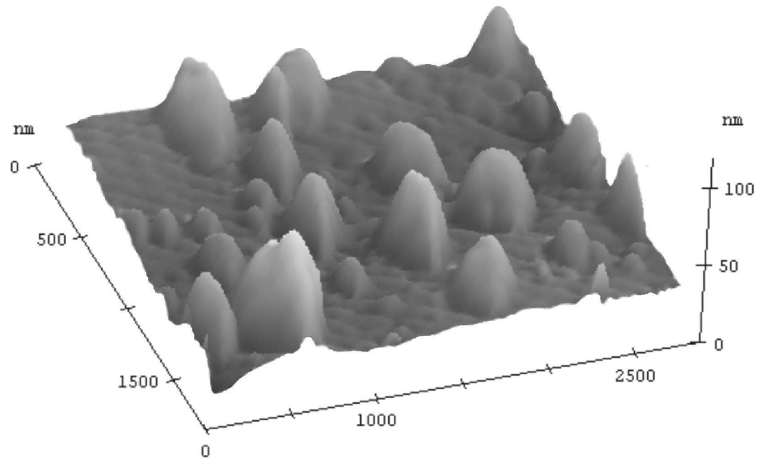

Figure 3. Space-picture of the $CsPbCl_3$ nanocrystals placed on the $Rb_{0.95}Cs_{0.05}Cl$-crystal cleavage surface.

4. Conclusions

Prolonged (t = 100 h) high-temperature (T = 200 °C) annealing of the $Rb_{0.95}Cs_{0.05}Cl$–Pb and $Rb_{0.8}Cs_{0.2}Cl$–Pb crystals with the structure of the NaCl type leads to the formation of the $CsPbCl_3$ nanocrystals dispersed in the corresponding matrix.

The formation of the $CsPbCl_3$ nanocrystals is confirmed by the manifestation of the quantum size effect which is displayed by a short-wave shift of the maximum of the excitonic luminescence emission of the $CsPbCl_3$ nanocrystals and by a shortening of the luminescent decay time from 0.48 ns in bulk single crystal to 0.15 ns in nanocrystals ($Rb_{0.95}Cs_{0.05}Cl$ matrix). The average radius of the nanocrystals determined from the magnitude of the quantum size energy is 2.8 nm for $Rb_{0.95}Cs_{0.05}Cl$–Pb and 4.7 nm for $Rb_{0.8}Cs_{0.2}Cl$–Pb.

The studies of the topology of the $Rb_{0.95}Cs_{0.05}Cl$–Pb crystal cleavage surface using the AFM method confirmed the fact of the formation of lead-containing nanocrystals.

The formation of the $CsPbCl_3$ nanocrystals embedded in wide gap matrices of $Rb_{1-x}Cs_xCl$ ($x = 0.05 \div 0.2$) solid solution with picosecond luminescent decay time does make it possible to develop fast detectors of high-energy irradiation. This circumstance demands the study of energy transfer processes from matrix to nanocrystals under excitation in the range of fundamental absorption of a matrix.

5. Acknowledgements

The authors are thankful to Professors M.V.Tkach, R.Levitskii and I.Bolesta for a discussion of experimental results. Partial support of INTAS (Grant 9901350) is also gratefully acknowledged.

References

1. Nikl M., Polak K., Nitsch K. et al. // Phys. Rev. B, 1995, vol. 51. p. 5192.
2. Myagkota S. // Optics and Spectroscopy, 1999, vol. 87, p. 311.
3. Voloshinovskii A., Myagkota S., Gloskovskii A., Gaba V. // J. Phys.: Condens. Matter, 2001, vol. 13, p. 8207
4. Myagkota S., Gloskovsky A., Voloshinovskii A. // Optics and Spectroscopy, 2000, vol. 88, p. 598.
5. Kulish M.R., Kunez V.P., Lysytsya M.P. // Ukr. J. Phys., 1996, vol. 41, No. 11–12, p. 1075 (in Ukrainian).
6. Somma F., Aloe P., Mastro Lo. et al. // J. Vac. Sci. Technol, 2001, vol. 19, p. 2237.
7. Nikl M., Nitsch K., Chval J. et al. // J. Phys.: Condens. Matter, 2001, vol. 12, p. 1939.
8. Somma F., Aloe P., Mastro Lo. et al. // Radiation Effects and Defects in Solids, 2001, vol. 156, p. 103.
9. Onodera Y., Toyozawa Y. // J. Phys. Soc. Japan, 1968, vol. 24, p. 341.
10. Nikl M., Polak K., Nitsch K. et al. // Radiation Effects and Defects in Solids, 1995, vol. 135, p. 288.

11. Apanasovich V.V., Novikov E.G. // Opt. Commun., 1991, vol. 78, p. 279.
12. Zimmerer G. // Nucl. instrum. Meth. Phys. Res. A, 1991, vol. 308, p. 178.
13. Efros Al.L., Efros A.L. // Fiz. Techn. Polupr., 1982, vol. 16, p. 1209 (in Russian)
14. Amitin L.N., Anistratov A.T., Kuznezov A.I. // Fiz. Tverd. Tela, 1979, vol. 21, p. 3535.
15. Pashuk I., Pidzyrailo N., Macko M. // Sol. Stat. Phys, 1981, vol. 23, p. 2162.
16. Kayanuma Y, Momiji U. // Phys. Rev. B, 1990, vol. 41, p. 10261
17. Voloshinovskii A., Myagkota S., Gloskovskii A., Zazubovich S. // Phys. Stat. Sol. (b), 2001, vol. 225, p. 257.

Люмінесцентно-кінетичні характеристики $CsPbCl_3$ агрегатів, диспергованих в матрицях $Rb_{1-x}Cs_xCl$ ($x = 0.05 \div 0.2$)

С.Мягкота, А.Глосковський, Р.Гладишевський, А.Волошиновський

Львівський національний університет ім. Івана Франка, 79005 Львів, вул. Кирила і Мефодія, 8

Отримано 21 квітня 2003 р.

Досліджено люмінесцентно-кінетичні параметри нанокристалів $CsPbCl_3$, диспергованих в матрицях твердих розчинів $Rb_{1-x}Cs_xCl$ ($x = 0.05 \div 0.2$). Утворення нанокристалів $CsPbCl_3$ підтверджується проявом квантово-розмірного ефекту, який реалізується в короткохвильовому зсуві максимума випромінювання екситонної люмінесценції і суттєвому скороченні часу загасання люмінесценції нанокристалів по відношенні до такого, характерного для смуги екситонної люмінесценції об'ємного монокристала $CsPbCl_3$.

Вперше з використанням методу атомно-силової мікроскопії здійснено пряме спостереження свинцевовмісних нанокристалів, вбудованих у матрицю кристалічного розчину $Rb_{0.95}Cs_{0.05}Cl$.

Ключові слова: *нанокристал, квантово-розмірний ефект, люмінесцентно-кінетичні параметри, морфологія кристалічного сколу, атомно-силова мікроскопія*

PACS: *32.50.+d, 87.15.Mi, 78.60.-b, 33.50.-j*